

## Article

# Structural Properties of Casein Micelles with Adjusted Micellar Calcium Phosphate Content

Elaheh Ahmadi <sup>1</sup>, Tatijana Markoska <sup>1</sup>, Thom Huppertz <sup>1,2,3</sup> and Todor Vasiljevic <sup>1,\*</sup>

<sup>1</sup> Advanced Food Systems Research Unit, Institute for Sustainable Industries and Liveable Cities, College of Sport, Health and Engineering, Victoria University, Melbourne, VIC 3001, Australia; elaheh.ahmadi@live.vu.edu.au (E.A.); tatijana.markoska@live.vu.edu.au (T.M.); thom.huppertz@wur.nl (T.H.)

<sup>2</sup> FrieslandCampina, 3818 LE Amersfoort, The Netherlands

<sup>3</sup> Food Quality and Design Group, Wageningen University and Research, 6708 WG Wageningen, The Netherlands

\* Correspondence: todor.vasiljevic@vu.edu.au

**Abstract:** Micellar calcium phosphate (MCP) content of skim milk was modified by pH adjustment followed by dialysis. Turbidity, casein micelle size and partitioning of Ca and caseins between the colloidal and soluble phases of milk were determined. Protein structure was characterised by Fourier transform infrared (FTIR) spectroscopy and proton nuclear magnetic resonance (<sup>1</sup>H NMR), whereas organic and inorganic phosphorus were studied by phosphorus-31 nuclear magnetic resonance (<sup>31</sup>P NMR). The sample with the lowest MCP content (MCP7) exhibited the smallest particle size and turbidity, measuring  $83 \pm 8$  nm and  $0.08 \pm 0.01$  cm<sup>-1</sup>, respectively. Concentrations of soluble caseins increased with decreasing MCP levels. At ~60% MCP removal, FTIR analysis indicated a critical stage of structural rearrangement and <sup>31</sup>P NMR analysis showed an increase in signal intensity for Ca-free Ser-P, which further increased as MCP concentration was further reduced. In conclusion, this study highlighted the importance of MCP in maintaining micellar structure and its impact on the integrity of casein micelle.

**Keywords:** micellar Ca phosphate; casein micelle; secondary structure of proteins; FTIR; NMR



**Citation:** Ahmadi, E.; Markoska, T.; Huppertz, T.; Vasiljevic, T. Structural Properties of Casein Micelles with Adjusted Micellar Calcium Phosphate Content. *Foods* **2024**, *13*, 322. <https://doi.org/10.3390/foods13020322>

Received: 29 December 2023

Revised: 18 January 2024

Accepted: 18 January 2024

Published: 19 January 2024



**Copyright:** © 2024 by the authors. Licensee MDPI, Basel, Switzerland. This article is an open access article distributed under the terms and conditions of the Creative Commons Attribution (CC BY) license (<https://creativecommons.org/licenses/by/4.0/>).

## 1. Introduction

Milk is a highly nutritious food containing both macronutrients, such as proteins (caseins and whey proteins) and fats, as well as micronutrients, including minerals such as Ca. The capacity of caseins to bind calcium in milk enables them to transport calcium and phosphate at concentrations significantly exceeding the solubility of calcium phosphate. This is possible because the majority of Ca and inorganic phosphate (P<sub>i</sub>) in milk is in the form of micellar calcium phosphate (MCP) within the casein micelles. Casein micelles are heterogeneous, dynamic, polydisperse spherical structures with an average diameter of 200 nm [1]. They are composed of the four caseins, α<sub>s1</sub>-, α<sub>s2</sub>-, β-, and κ-casein, which are connected via various intermolecular interactions, as well as via MCP nanoclusters that connect to caseins via phosphoserines located on the former three caseins. The dry matter of the casein micelle consists of ~94% protein and ~6% inorganic material [2].

Of the total Ca content in bovine milk, ~70% is found in the casein micelles (protein-bound Ca, micellar) and ~30% is found in the serum phase (diffusible Ca) [3]. Serum Ca is partially present in ionic form, but also as complexes with citrate and phosphate ions. Conditions such as temperature, pH, as well as the addition of Ca-sequestering salts (CSS) can alter the amount of MCP, but also affect the Ca species in the serum phase. Alteration of the MCP level of the casein micelles can affect the structure and properties of casein micelles, which may further broaden the application range for milk protein ingredients in the food, cosmetic, and medicine domains [3].

The amount of soluble calcium affects rennetability, thermal stability, and rheological properties of various dairy products thus, calcium reduction was proposed as a way to improve the functionality of various dairy products. Due to the requirement for specific techno-functional properties of caseins as well as their nutritional benefits, in recent years, various studies have been conducted and different process options for calcium reduction in skim milk were compared quantitatively and qualitatively to produce casein micelles with an altered MCP content, e.g., in skim milk retentates [4] and in milk [5–11]. While functional properties of MCP-adjusted milks, such as thermal stability [12–14] and digestion [10] have been studied in detail, detailed studies on MCP-adjusted casein micelles have been more limited and the secondary structure of the proteins in MCP-adjusted skim milk was not investigated. This study aimed to investigate how modifying the MCP content in skim milk influences the structural characteristics of casein micelles, specifically focusing on its impact on micellar integrity.

## 2. Materials and Methods

### 2.1. Materials

Freshly pasteurised skim milk was sourced from Warrnambool Cheese and Butter—Saputo in Warrnambool, Victoria, Australia. Sodium azide (0.02%, *w/w*), glucono-delta-lactone (GDL), sodium hydroxide (NaOH), deuterium oxide (D<sub>2</sub>O) and Pronase (protease mixture) were procured from Sigma-Aldrich in St. Louis, MO, USA. Additionally, high retention seamless cellulose dialysis tubing (14 kDa MWCO) was obtained from Sigma-Aldrich, St. Louis, MO, USA.

### 2.2. Sample Preparation

Samples were prepared from freshly pasteurised skim milk obtained from Warrnambool Cheese and Butter—Saputo (Warrnambool, Victoria, Australia) on three separate occasions. To prevent bacterial growth, sodium azide (0.02%, *w/w*) was added to the milk on receipt. In order to prepare samples varying in MCP content, the skim milk was subjected to a protocol described previously [5], whereby pH of skim milk was first either lowered to 4.9, 5.5, 5.7, 5.8, 5.9 or 6.1 by the addition of predetermined amounts of glucono-delta-lactone (GDL) or increased to 7.5 or 8.2 by adding 1.0 M NaOH at 5 °C. After the pH was stabilised, the pH-adjusted samples, as well as a control sample maintained at pH 6.7, were dialysed using a high retention seamless cellulose dialysis tubing (14 kDa MWCO, Sigma-Aldrich, St. Louis, MO, USA), against 2 × 20 volumes of original pasteurised skim milk for 72 h at 5 °C [5,10]. After the dialysis, the samples were removed from dialysis tubing and analysed. The study design of the present study and associated sample coding is shown in Figure 1. The coding was based on the estimate of micellar Ca relative to that of the control. Micellar Ca was defined as the amount of Ca that sedimented on ultracentrifugation (Section 2.3).

### 2.3. Sample Fractionation

The sedimentable and non-sedimentable phase of milk samples were separated by ultracentrifugation at 100,000 × *g* for 1 h at 20 °C using a Beckman Ultra L-70 centrifuge (Beckman Coulter, Australia Pty. Ltd., Gladesville, Australia). The clear supernatant was then collected carefully with a syringe from each tube. To prepare 10 kDa-permeable fractions, part of the ultracentrifugal supernatant was subsequently filtered through a centrifugal 10 kDa filter at 4000 × *g* for 4 h (Corning Spin-X UF concentrators, Merck, Darmstadt, Germany) using an Eppendorf Model 5810 centrifuge (Hamburg, Germany). A 10 kDa-permeable fraction was also prepared, similar to outlined above, from milk samples which had been incubated with 0.4 mg mL<sup>−1</sup> of the protease mixture Pronase from *Streptomyces griseus* type XIV (Sigma-Aldrich, ST. Louis, MO, USA) for 24 h at 20 °C.

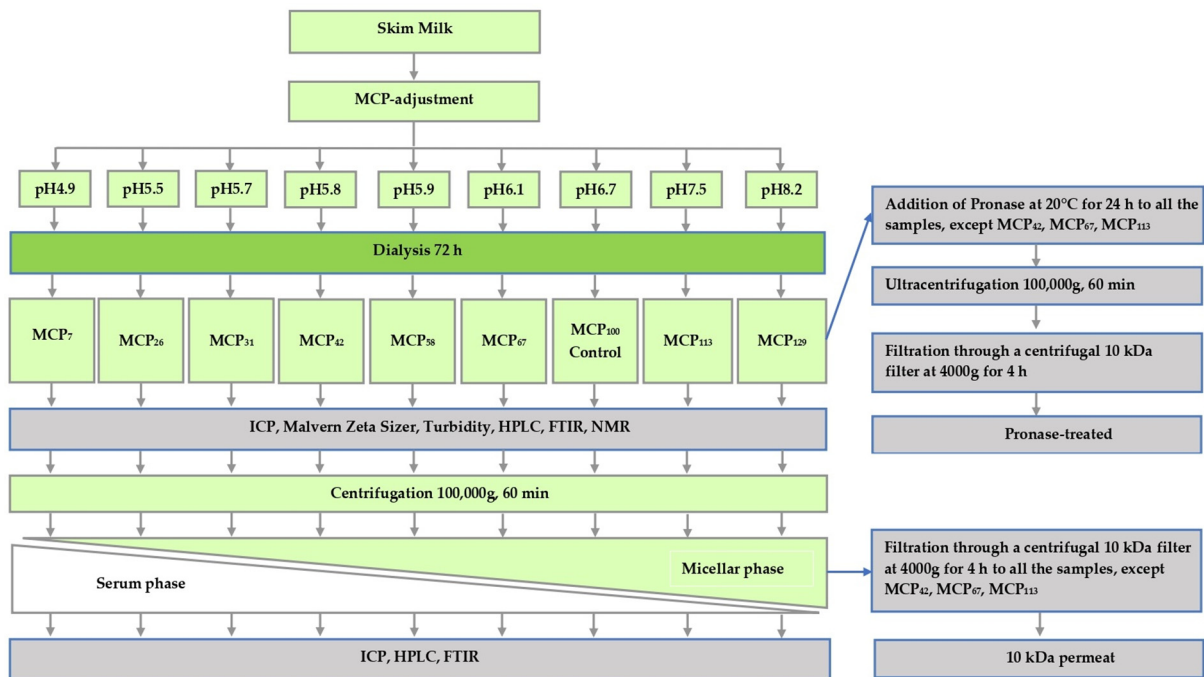


**Figure 1.** Experimental design of this study.

## 2.4. Sample Analysis

### 2.4.1. Ca Determination

The concentration of Ca in the whole samples, ultracentrifugal supernatant, and the 10 kDa permeates of milk with and without prior pre-treatment with Pronase was determined using an inductively coupled plasma atomic emission spectrometer (ICP-AES, ICPE-9000 system, Shimadzu Corporation, Kyoto, Japan) [15]. Micellar Ca was defined as the amount of sedimentable Ca (i.e., total Ca–Ca in the ultracentrifugal supernatant). The amount of nanocluster-associated Ca was determined as the difference between total Ca and the amount of Ca in the 10 kDa permeate of Pronase-treated milk.

### 2.4.2. Particle Size Distribution and Turbidity

Particle size (Z-average diameter) was determined by dynamic light scattering (Zetasizer-Nano, Malvern instruments Ltd., Malvern, UK) at a scattering angle of 90° at 25° C. Samples were diluted in simulated milk ultrafiltrate (SMUF) [16] in a ratio of 1:100. Refractive indexes for casein micelle and SMUF of 1.57 and 1.342, respectively, were used [17]. Turbidity of the bulk samples was measured at 860 nm using 1 mm path length quartz cuvettes using a UV–Visible spectrophotometer (Biochrom Ltd., Cambridge, UK) following the previously described method [15]. Turbidity of the milk serum after centrifugation was also measured.

### 2.4.3. High-Performance Liquid Chromatography

Caseins in whole samples and ultracentrifugal supernatants were analysed using a reversed-phase high-performance liquid chromatography (RP-HPLC) at room temperature by a Shimadzu HPLC system (Model Prominence-i, LC-2030 C, Shimadzu Corporation, Kyoto, Japan) with a Varian 9012 system controller (Agilent Technologies Inc., Santa Clara, CA, USA) coupled with a RI detector (Varian, 9050) and a C<sub>4</sub> column (Aeris Widepore, 150 mm × 4.6 mm, 3.6 µm particle size, 300 Å porosity, Phenomenex, Torrance, CA, USA). Samples were prepared and analysed according to the method described previously [15].

### 2.4.4. Fourier Transform Infrared (FTIR) Spectroscopy

For FTIR spectroscopy measurements, all milk samples were analysed using an FTIR spectrometer (Frontier 1, PerkinElmer, Boston, MA, USA) in the range of 4000–600 cm<sup>-1</sup>.

At the start of measurement, the background spectrum was scanned with a blank (SMUF) to resolve changes in milk proteins [18]. In addition, corresponding ultracentrifugal supernatant samples were analysed under the same instrumental conditions as for the milk sample spectra acquisition [18]. The spectrum of ultracentrifugal supernatants was subtracted from corresponding spectrum of milk samples to reveal structural features of the micellar casein fraction. In the Amide I band region of the FTIR spectra between 1700 and 1600  $\text{cm}^{-1}$ , six features corresponding to main protein secondary structures were assigned: side chains (1608–1611  $\text{cm}^{-1}$ ),  $\beta$ -sheet (1620–1631  $\text{cm}^{-1}$ ), random coils (1640–1649  $\text{cm}^{-1}$ ),  $\alpha$ -helix (1658–1666  $\text{cm}^{-1}$ ),  $\beta$ -turns (1668–1681  $\text{cm}^{-1}$ ), and aggregated  $\beta$ -sheet (1689–1694  $\text{cm}^{-1}$ ) [19]. By subtracting the supernatants from the corresponding bulk samples, the aim was to visualise the changes associated with the micellar casein phase.

#### 2.4.5. NMR Spectroscopy

NMR analysis was carried out using a 600 MHz Bruker Avance spectrometer (Bruker BioSpin GmbH, Rheinstetten, Germany). For the  $^{31}\text{P}$  NMR analysis, the samples were prepared by mixing 0.1 mL of deuterium oxide and 0.9 mL of milk sample, whereas for the  $^1\text{H}$  NMR analysis the samples were mixed by 0.9 mL of deuterium oxide 10% and 0.1 mL of milk. The  $^1\text{H}$  NMR spectra were recorded using 32 scans and spectral width of 9615 Hz. The water signal was suppressed using excitation sculpting with gradients allowing for presaturation during relaxation delay in cases of radiation damping [19]. The  $^{31}\text{P}$  NMR spectra were acquired at frequency of 242 MHz with power-gated proton decoupling, acquisition time of 0.3 s and 36 number of scans. The spectra were analysed using TopSpin 4.1.1 software (Bruker BioSpin). The FID was corrected by 0.3 Hz line-broadening parameter and phase correction by 0th and 1st order correction for pk. For both analyses,  $^1\text{H}$  and  $^{31}\text{P}$  NMR, each sample was analysed in triplicate.

#### 2.5. Statistical Analysis

All experiments assessed the impact of MCP content on the selected parameters. SPSS software v. 26 (IBM Inc. Chicago, IL, USA) was used for one-way analysis of variance (ANOVA) to establish differences among means followed by Tukey's multicomparison of the means. The level of significance was pre-set at  $p < 0.05$ . The data were replicated three times on three different occasions. In addition, the FTIR data, processed as described previously, was analysed by Principal Component Analysis (PCA) with Origin Pro 2021, v. 95E software (OriginLab Corporation, Northampton, MA, USA), as described previously [18].

### 3. Results

#### 3.1. Ca Distribution

Table 1 shows the concentrations of Ca in the different fractions of MCP-adjusted skim milk samples. The total Ca content of the control skim milk (MCP<sub>100</sub>) was  $\sim 32.2 \text{ mmol L}^{-1}$ , out of which  $21.5 \text{ mmol L}^{-1}$  was colloidal,  $10.7 \text{ mmol L}^{-1}$  was found in the ultracentrifugal supernatant and  $9.7 \text{ mmol L}^{-1}$  was 10 kDa permeable. Concentrations of Ca in the ultracentrifugal supernatants were slightly higher than the corresponding levels in the 10 kDa-permeable fractions, due to fact that whey proteins and caseins in the ultracentrifugal supernatant bind some Ca. In agreement with previous studies [5,10], MCP levels decreased in samples that were dialysed after acidification, whereas it increased in samples that were alkalised prior to dialysis (Table 1). In addition to micellar Ca, we also estimated nanocluster-associated Ca, as previous studies indicated that not all micellar Ca is in the MCP nanoclusters [20]. To do this, the level of Ca in the 10 kDa-permeable fraction of milk that treated with Pronase was determined.

**Table 1.** Ca concentration in milk, its supernatant (100,000 × g for 60 min), 10 kDa permeate and the 10 kDa permeate of milk after treatment with Pronase for pasteurised skim milk samples with their MCP adjusted to 7% (MCP<sub>7</sub>) to 129% (MCP<sub>129</sub>) by either acidification or alkalisation followed by exhaustive dialysis against bulk milk. MCP content was relative to the control based on the nanocluster associated Ca.

Sample Code <sup>1</sup>	pH of Milk Prior to Dialysis	Total Ca (mmol L <sup>-1</sup> )	Supernatant Ca (mmol L <sup>-1</sup> )	10 kDa Permeable Ca (mmol L <sup>-1</sup> )	10 kDa-Permeable Ca of Pronase-Treated Milk (mmol L <sup>-1</sup> )	Nanocluster-Associated Ca (mmol L <sup>-1</sup> )
MCP <sub>7</sub>	4.9	14.74 ± 1.01 <sup>E</sup>	13.24 ± 0.50 <sup>A</sup>	12.49 ± 0.26 <sup>A</sup>	12.65 ± 1.56	2.09 ± 0.06 <sup>F</sup>
MCP <sub>26</sub>	5.5	18.24 ± 3.19 <sup>DE</sup>	12.53 ± 2.19 <sup>AB</sup>	11.48 ± 0.94 <sup>AB</sup>	13.54 ± 1.38	4.70 ± 0.20 <sup>E</sup>
MCP <sub>31</sub>	5.7	19.23 ± 5.06 <sup>DE</sup>	12.51 ± 2.30 <sup>AB</sup>	11.64 ± 0.53 <sup>AB</sup>	12.84 ± 1.33	6.39 ± 0.09 <sup>D</sup>
MCP <sub>42</sub>	5.8	21.38 ± 3.42 <sup>CD</sup>	12.32 ± 2.07 <sup>AB</sup>	N/A	N/A	N/A
MCP <sub>58</sub>	5.9	23.68 ± 3.38 <sup>CD</sup>	11.08 ± 0.72 <sup>AB</sup>	11.49 ± 2.38 <sup>AB</sup>	13.21 ± 1.14	10.47 ± 0.06 <sup>C</sup>
MCP <sub>67</sub>	6.1	25.42 ± 1.55 <sup>C</sup>	10.92 ± 0.87 <sup>AB</sup>	N/A	N/A	N/A
MCP <sub>100</sub>	6.7	32.23 ± 1.79 <sup>B</sup>	10.72 ± 0.67 <sup>AB</sup>	9.78 ± 0.09 <sup>B</sup>	11.72 ± 2.33	20.51 ± 0.02 <sup>B</sup>
MCP <sub>113</sub>	7.5	35.43 ± 2.83 <sup>AB</sup>	11.04 ± 0.48 <sup>AB</sup>	N/A	N/A	N/A
MCP <sub>129</sub>	8.2	38.17 ± 3.19 <sup>A</sup>	10.47 ± 0.28 <sup>B</sup>	11.63 ± 1.58 <sup>AB</sup>	13.92 ± 1.57	24.25 ± 0.10 <sup>A</sup>

<sup>1</sup> The subscript numbers indicate proportion of retained MCP relative to that of the control; The superscript capital letters indicate significant differences within the rows across treatment by Tukey's honestly significant difference procedure ( $p < 0.05$ ); results are expressed as the means ± standard deviation; N/A—not assessed.

Treatment of milk with this enzyme mixture is known to hydrolyse milk proteins to free amino acids and small peptides, which can permeate through a 10 kDa membrane, whereas the Ca phosphate nanoclusters remain intact [21,22]. Hence, Ca associated with other parts of the caseins would permeate through the 10 kDa membrane after hydrolysis with Pronase. Using this approach, the concentration of nanocluster-associated Ca was estimated to be 20.5 mmol L<sup>-1</sup> in the control milk. With decreasing MCP content, the concentration of nanocluster-associated Ca decreased significantly, down to 2 mmol L<sup>-1</sup> of the nanocluster associated Ca for sample MCP<sub>7</sub> (Table 1).

### 3.2. Physicochemical Properties of Skim Milk with the Altered MCP Content

Particle size and turbidity of all samples are presented in the Table 2, whereas the particle size distribution of the milk samples is shown in Figure 2. The average particle size in control skim milk was 163 nm (Table 2), in line with previous reports [10]. With decreasing MCP content, the turbidity of skim milk samples decreased progressively, with the turbidity of the sample MCP<sub>7</sub> close to that of the milk serum (Table 2), indicating a very high degree of disintegration of the casein micelle. On the other hand, increasing the MCP content did not alter the turbidity (Table 2).

**Table 2.** Particle diameter and turbidity for pasteurised skim milk samples with their MCP adjusted from 7% (MCP<sub>7</sub>) to 129% (MCP<sub>129</sub>) by either acidification or alkalisation followed by exhaustive dialysis against bulk milk For sample details, see Figure 1.

Sample	Particle Diameter (nm)	Turbidity (cm <sup>-1</sup> )
MCP <sub>7</sub>	83 ± 8 <sup>D</sup>	0.08 ± 0.01 <sup>I</sup>
MCP <sub>26</sub>	115 ± 7 <sup>C</sup>	0.14 ± 0.01 <sup>H</sup>
MCP <sub>31</sub>	140 ± 17 <sup>B</sup>	0.23 ± 0.00 <sup>G</sup>
MCP <sub>42</sub>	158 ± 14 <sup>A</sup>	0.26 ± 0.00 <sup>F</sup>
MCP <sub>58</sub>	163 ± 8 <sup>A</sup>	0.29 ± 0.00 <sup>E</sup>
MCP <sub>67</sub>	162 ± 5 <sup>A</sup>	0.32 ± 0.00 <sup>D</sup>
MCP <sub>100</sub> (control)	163 ± 4 <sup>A</sup>	0.41 ± 0.00 <sup>A</sup>
MCP <sub>113</sub>	169 ± 11 <sup>A</sup>	0.40 ± 0.00 <sup>B</sup>
MCP <sub>129</sub>	165 ± 5 <sup>A</sup>	0.39 ± 0.00 <sup>C</sup>

The capital letters indicate significant differences within the rows across treatment by Tukey's honestly significant difference procedure ( $p < 0.05$ ); results are expressed as the means ± standard deviation.

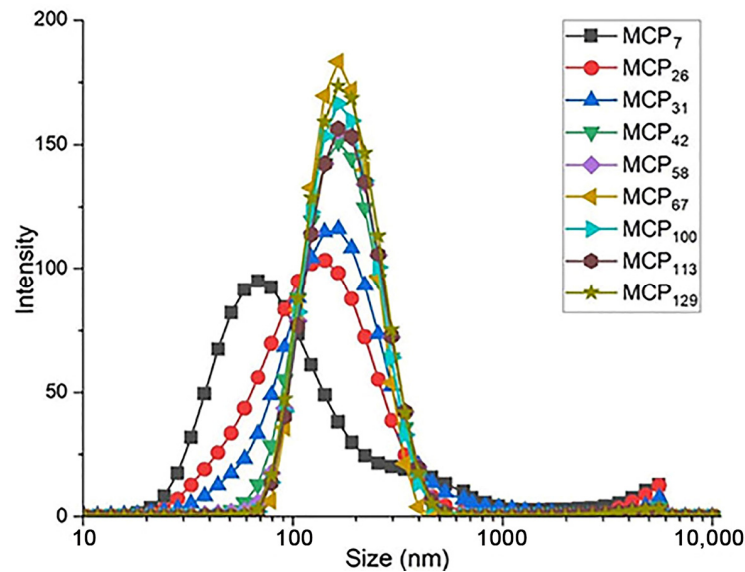


**Figure 2.** Particle size distribution of MCP modified skim milk samples. MCP content was adjusted from 7% (MCP<sub>7</sub>) to 129% (MCP<sub>129</sub>) relative to the control by either acidification or alkalisation followed by exhaustive dialysis against bulk milk. Graph is representative of two replicate samples.

### 3.3. Distribution of Individual Caseins in the MCP-Adjusted Skim Milk

Results for the protein composition of the ultracentrifugal supernatants of the MCP-adjusted skim milk samples as determined by HPLC are shown in Figure 3. The percentage of non-sedimentable  $\alpha_{S1}$ - $\alpha_{S2}$ -,  $\kappa$ -, and  $\beta$ -casein increased with decreasing MCP content (Figure 3), particularly from sample MCP<sub>67</sub>. The highest concentrations of non-sedimentable caseins were found in sample MCP<sub>7</sub>. Increasing the MCP content caused slight decrease in the concentrations of individual soluble caseins in comparison to the control (MCP<sub>100</sub>) (Figure 3). Comparable trends were observed for all caseins.

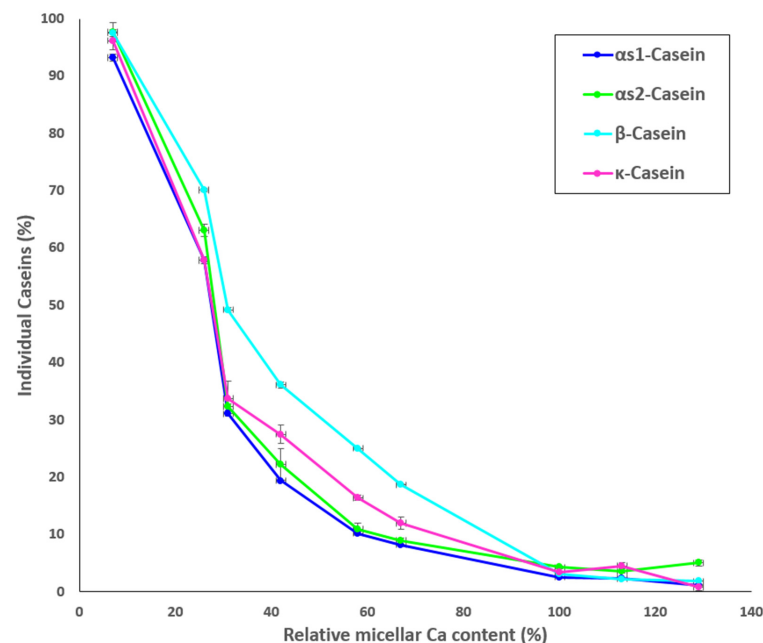


**Figure 3.** Proportion (%) of individual caseins present in the supernatant to skim milk as a function of the relative micellar Ca content, calculated as a ratio of micellar Ca content of a sample after pH adjustment and dialysis to micellar Ca content of the control.

### 3.4. Structural Characterisation of MCP Adjusted Skim Milk Samples by FTIR

The structural changes in the Amide I region of milk proteins and the micellar casein fraction in the samples are shown in Table S1 and Table 3, respectively. FTIR spectra in the region between 4000 and 650  $\text{cm}^{-1}$  are presented in Figure S1. The most substantial difference as a result of adjusting the MCP content of skim milk was observed in the side chains of the amino acids (1608–1611  $\text{cm}^{-1}$ ), with the greatest intensity observed for samples MCP<sub>113</sub> and MCP<sub>129</sub> (Table S1; Table 3). The intensity of side chains in the micellar casein fraction decreased significantly at two key points when MCP content was reduced (Table 3). The first notable decrease was observed between samples MCP<sub>100</sub> and MCP<sub>67</sub>, and the second significant change was observed between samples MCP<sub>58</sub> and MCP<sub>42</sub> (Table 3). It is important to note that the side chains of amino acids can contribute to the structural integrity of proteins through weak interactions, such as ionic or hydrogen bonds [23].

**Table 3.** Changes in structural features of individual caseins in Amide I region of MCP-adjusted skim milk samples as determined by Fourier transform Infrared Spectroscopy. MCP-adjusted skim milk samples containing from 7% (MCP<sub>7</sub>) to 129% (MCP<sub>129</sub>) of MCP relative to that of the control were obtained by either acidification or alkalisation followed by exhaustive dialysis against bulk milk. The spectra were obtained after the background adjustment using the corresponding supernatants obtained by ultracentrifugation.

Band Assessment	Side Chain	$\beta$ -Sheet	Random Coil	$\alpha$ -Helix	$\beta$ -Turn	Aggregated $\beta$ -Sheet
Band Frequency ( $\text{cm}^{-1}$ )	1608–1611	1620–1631	1640–1649	1658–1666	1668–1681	1689–1694
MCP <sub>7</sub>	1.1 $\pm$ 0.02 <sup>g</sup>	11.8 $\pm$ 0.20 <sup>ab</sup>	16.9 $\pm$ 1.34 <sup>a</sup>	24.2 $\pm$ 1.88 <sup>abc</sup>	44.8 $\pm$ 0.98 <sup>ab</sup>	1.2 $\pm$ 0.21 <sup>ef</sup>
MCP <sub>26</sub>	1.9 $\pm$ 0.23 <sup>fg</sup>	6.6 $\pm$ 0.35 <sup>d</sup>	15.0 $\pm$ 2.28 <sup>ab</sup>	21.6 $\pm$ 0.49 <sup>bc</sup>	52.3 $\pm$ 2.20 <sup>a</sup>	2.4 $\pm$ 0.13 <sup>def</sup>
MCP <sub>31</sub>	3.8 $\pm$ 0.11 <sup>e</sup>	6.7 $\pm$ 0.03 <sup>d</sup>	11.4 $\pm$ 0.59 <sup>ab</sup>	22.5 $\pm$ 0.03 <sup>bc</sup>	52.0 $\pm$ 0.02 <sup>a</sup>	3.5 $\pm$ 0.43 <sup>de</sup>
MCP <sub>42</sub>	2.3 $\pm$ 0.09 <sup>f</sup>	1.9 $\pm$ 0.33 <sup>e</sup>	13.9 $\pm$ 1.27 <sup>ab</sup>	33.3 $\pm$ 1.72 <sup>a</sup>	48.4 $\pm$ 2.76 <sup>ab</sup>	0.1 $\pm$ 0.02 <sup>f</sup>
MCP <sub>58</sub>	9.5 $\pm$ 0.45 <sup>d</sup>	3.2 $\pm$ 0.33 <sup>e</sup>	9.9 $\pm$ 0.42 <sup>b</sup>	23.5 $\pm$ 1.81 <sup>bc</sup>	50.6 $\pm$ 2.75 <sup>a</sup>	2.9 $\pm$ 0.42 <sup>de</sup>
MCP <sub>67</sub>	10.3 $\pm$ 0.03 <sup>d</sup>	9.8 $\pm$ 0.67 <sup>bc</sup>	11.9 $\pm$ 3.61 <sup>ab</sup>	30.5 $\pm$ 1.09 <sup>ab</sup>	34.0 $\pm$ 5.57 <sup>cd</sup>	4.8 $\pm$ 0.03 <sup>d</sup>
MCP <sub>100</sub>	15.2 $\pm$ 0.28 <sup>c</sup>	6.9 $\pm$ 2.09 <sup>cd</sup>	11.1 $\pm$ 1.57 <sup>ab</sup>	15.1 $\pm$ 6.27 <sup>c</sup>	40.8 $\pm$ 0.54 <sup>bc</sup>	10.8 $\pm$ 1.80 <sup>c</sup>
MCP <sub>113</sub>	32.6 $\pm$ 0.18 <sup>a</sup>	13.2 $\pm$ 0.18 <sup>a</sup>	10.1 $\pm$ 0.22 <sup>b</sup>	2.6 $\pm$ 0.10 <sup>d</sup>	21.9 $\pm$ 0.05 <sup>e</sup>	19.5 $\pm$ 0.37 <sup>b</sup>
MCP <sub>129</sub>	24.1 $\pm$ 0.42 <sup>b</sup>	6.5 $\pm$ 0.02 <sup>d</sup>	17.2 $\pm$ 0.13 <sup>a</sup>	2.8 $\pm$ 0.00 <sup>d</sup>	26.7 $\pm$ 0.25 <sup>de</sup>	22.7 $\pm$ 0.29 <sup>a</sup>

The subscripts indicate proportion of retained MCP relative to that of the control; The small letters show significant differences within the columns ( $p < 0.05$ ); the results are expressed as the means  $\pm$  standard deviation.

The greatest structural changes could be assigned to the micellar casein fraction. The proportion of side chains, which contribute to the structural integrity of proteins through weak interactions, such as ionic or hydrogen bonds [23], was greatest at the MCP level above that of the control, it however consistently declined concomitant with the reduction in the MCP content. On the contrary, the proportion of  $\beta$ -turns followed an inversed pattern to that of the side chains with the lowest values obtained at high MCP content. Random coil and  $\beta$ -sheet structures, with some exceptions, remained fairly consistent across the whole MCP range (Table 3).  $\alpha$ -Helical structures significantly increased when lowering MCP content down to 42% of the original level, after which it declined by almost 30% (Table 3). At the same time, contributions of the  $\beta$ -sheet and aggregated  $\beta$ -sheet structures were the lowest for MCP<sub>42</sub>.

From these observations, sample MCP<sub>42</sub> appeared to be a key point at which the structural components of the proteins underwent substantial changes as a result of changes in the MCP content. PCA analysis also confirmed differences in structural components in Amide I region based on MCP-adjustment, classifying the samples into three groups (Figure 4). The PC1 differentiated the MCP adjusted skim milk samples in three groups including the MCP-enriched samples (MCP<sub>113</sub> and MCP<sub>129</sub>) from the low-MCP samples (MCP<sub>7</sub>–MCP<sub>58</sub>), and samples MCP<sub>67</sub>–MCP<sub>100</sub> (Figure 4).

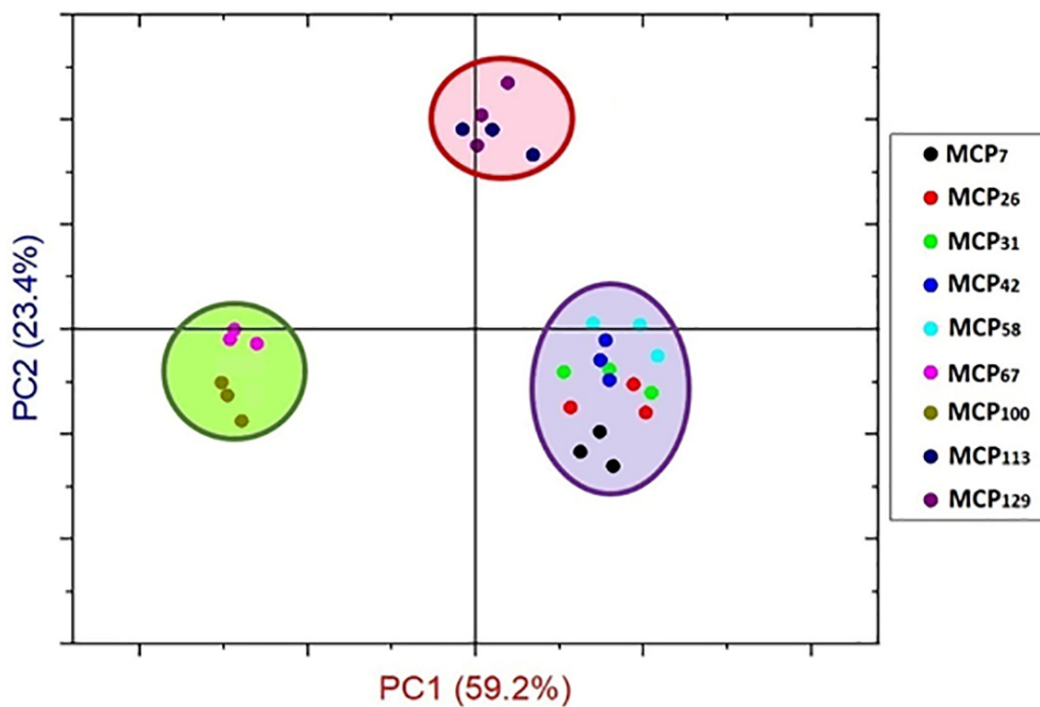


**Figure 4.** Principal component scores for Amide I region ( $1700\text{--}1600\text{ cm}^{-1}$ ) of MCP-adjusted skim milk samples containing from 7% (MCP<sub>7</sub>) to 129% (MCP<sub>129</sub>) of MCP relative to that of the control achieved by either acidification or alkalinisation followed by exhaustive dialysis against bulk milk.

#### H and <sup>31</sup>P NMR

The MCP-adjusted milk samples were analysed by <sup>31</sup>P and <sup>1</sup>H NMR spectroscopy. The <sup>31</sup>P NMR spectra provide information on the changes in the state of phosphate in milk and the spectra presented in Figure 5 are characterised by two distinct peaks, one narrow peak at  $\delta = 1\text{--}1.5$  ppm assigned to P<sub>i</sub> and a broader peak at around 3 ppm usually assigned to P<sub>o</sub>. In the control samples, the P<sub>o</sub> signal at 2.0–3.5 ppm was very broad and started to become more prominent at MCP<sub>42</sub> (Figure 5D) with the greatest intensity detected at MCP<sub>7</sub> (Figure 5A). The signal shape and intensity of this peak depends on the different chemical environments and mobility of SerP [24], with the signal disappearing concomitant with the phosphorus immobilisation. The P<sub>o</sub> signal appeared to be noticeably different for the samples containing the least amount of MCP (Figure 5A–C), whereas the P<sub>i</sub> peak appeared consistently across these ranges of MCP. The width of the P<sub>i</sub> peak is impacted by the MCP concentration; in samples with higher MCP content (Figure 5H,I), a broader width is observed.

The <sup>1</sup>H NMR spectra showed an intense signal for lactose at 3.2–4.0 ppm (Figure 6) [25]. Signal intensity in the aliphatic region (0.5–2.0 ppm) decreased as the MCP concentration was increased. The methyl signal that appears at ~0.5 ppm was most intense in MCP<sub>7</sub> and the least in MCP<sub>129</sub> (Figure 6). This resonance arises from the methyl protons of alanine, leucine, isoleucine and threonine and their intensity could be related to their greater presence in the soluble phase [26]. Similarly, the aromatic region of the spectrum (6–9 ppm) [27], depicting ring protons of phenylalanine, tyrosine, tryptophan and histidine, resonated greatly at lower MCP content (Figure 6A–E), which again was attributed to a greater proportion of soluble proteins in the past [28]. The H $\alpha$  and H $\beta$  regions of the <sup>1</sup>H NMR spectra also showed variation in the signal intensity when the MCP concentration was altered (Figure 6). Changes were observed in the doublet at 2.5 ppm, doublet at 3.0 ppm, singlet at 4.2 ppm, singlet at 5.2 ppm and multiple signals at 4.7 ppm. The chemical shifts in the MCP<sub>31</sub> sample at 2.5, 3.0, 4.2 and 5.2 ppm show lower signal intensity compared to the rest of the samples. Thus, the signal in this region could be due to involvement in hydrogen

interactions guided by the H $\alpha$  and H $\beta$  of the backbone. The signals at 4.7 ppm could not be interpreted accurately as the water suppression interfered with the signal intensity.

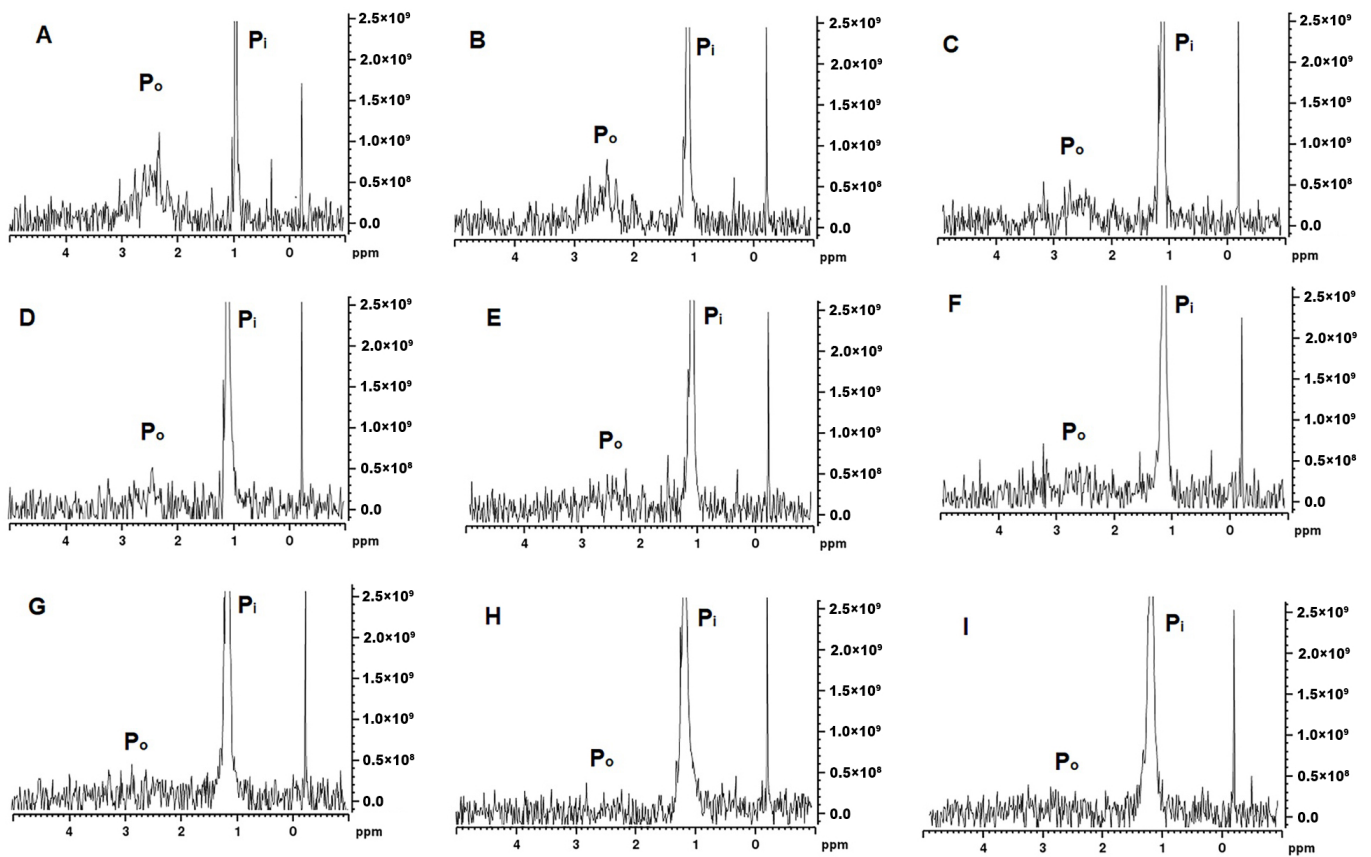


**Figure 5.**  $^{31}\text{P}$  NMR spectra for MCP $_7$  (A), MCP $_{26}$  (B), MCP $_{31}$  (C), MCP $_{42}$  (D), MCP $_{58}$  (E), MCP $_{67}$  (F), MCP $_{100}$  (G), MCP $_{113}$  (H), and MCP $_{129}$  (I).

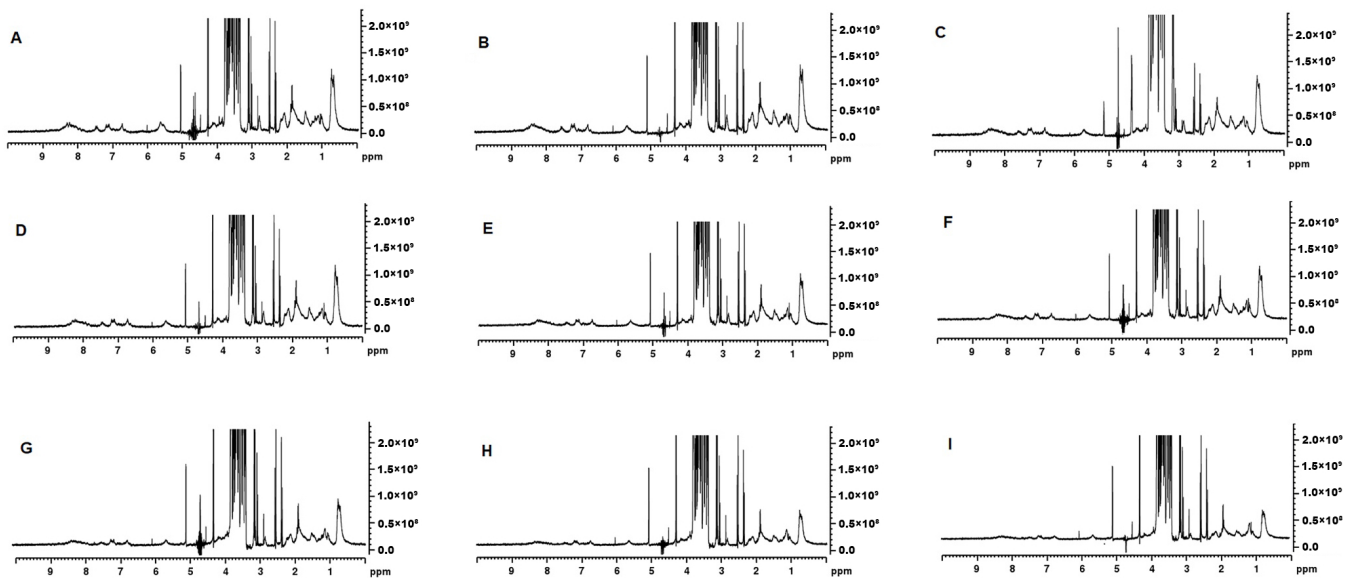


**Figure 6.**  $^1\text{H}$  NMR spectra for MCP $_7$  (A), MCP $_{26}$  (B), MCP $_{31}$  (C), MCP $_{42}$  (D), MCP $_{58}$  (E), MCP $_{67}$  (F), MCP $_{100}$  (G), MCP $_{113}$  (H), and MCP $_{129}$  (I).

## 4. Discussion

### 4.1. Impact of Micellar Calcium Phosphate Levels on the Casein Micelle Structure

Casein micelles are in a dynamic equilibrium with the surrounding serum; thus, they can exchange proteins and minerals under various saturation conditions, and rearrange their structure in different chemical environments [29]. De Kruijff et al. [30] showed that the previously proposed nanocluster model [31] captures the main features of the casein micelle. In this model, the MCP is dispersed by competent phosphopeptides to form equilibrium core-shell nanoclusters [20]. Based on this model, phosphorylated caseins bind to the growing nanoclusters [30]. The proteins associated with the nanoclusters protrude out and interact with other proteins via weak interactions, including hydrophobic interactions, hydrogen bonding, ion bonding and weak electrostatic interactions, which results in formation of a more or less homogeneous protein matrix [30]. Previously, Holt et al. [32] stated that micellar Ca appears to exist in two forms—as a Ca phosphate salt and as  $\text{Ca}^{2+}$  bound to the protein. Similarly, originally it was believed that phosphorus appeared in 2 chemical forms in casein micelle: as the MCP and phosphorylated serine (phosphoserine) in the caseins [33,34]. However, more recently Hindmarsh and Watkinson showed using  $^1\text{H}$   $^{31}\text{P}$  cross-polarisation magic angle spinning (CP-MAS) NMR that in addition to these two forms, other immobile phosphorus bodies exist within the casein micelle that have not yet been classified [35].

### 4.2. Micellar Calcium Phosphate Adjustment: Insights from FTIR Analysis

The state of MCP has a notable effect on the properties of the casein micelle. The results of the current study confirmed previous findings [8–10,15] that the MCP adjustment changes Ca equilibrium (Table 1), resulting in a substantial decline of the average particle size below  $\text{MCP}_{42}$ . Interestingly, from the data in Table 2 it seems that turbidity declined almost linearly with decreasing MCP content. The caseins and MCP are responsible for the light-scattering properties of the casein micelle [36] thus decreasing MCP concentration reduces the refractive index of the casein micelles, and thus turbidity of the milk. However, a decrease in turbidity was also associated with a release of individual caseins [2], which indicated changes in the concentration of non-sedimentable caseins in the serum phase (Figure 3).  $\beta$ -Casein appeared to be the most affected micellar protein initially, with almost 40% of its initial micellar concentration released into the serum (Figure 3). This could be related to its positioning in the casein micelle, as some studies indicated that  $\beta$ -casein may either be present or be close to the surface [37,38]. The role of MCP in maintaining  $\beta$ -casein association with the micelle was also linked to its greater solubility at low temperature [39].

Structurally, the main changes observed were associated with the micellar and the non-sedimentable caseins. Only limited changes in structural elements took place when all milk proteins were assessed involving side chains,  $\beta$ -sheets and random coils while  $\alpha$ -helix,  $\beta$ -turns and aggregated  $\beta$ -sheets remained fairly consistent (Table S1). Changes were likely influenced by dissociation of individual caseins from the micelle, as whey proteins likely remain unaffected by the whole process of MCP adjustment. On the other hand, the casein micelle underwent substantial structural changes (Table 3), with changes becoming very prominent around residual MCP content of 42 to 58% of the original. The Amide I signal of the casein micelle was previously reported to contain ~40% of  $\beta$ -turns at the natural pH of milk [40], similar to what was observed in the current study (Table 3). The substantial increase of  $\beta$ -turns upon the MCP reduction could in part be attributed to dissolution of  $\beta$ -casein from the micelle since it contains approximately 20% of  $\beta$ -turns [40,41]. In addition,  $\beta$ -casein contains a large proportion of  $\beta$ -sheets [41] thus the decline in this structural feature of the casein micelle could have been caused also by the  $\beta$ -casein solubilisation. Considering other physical properties, it is likely that the structure of the casein micelle remains fairly stable up to a certain point, around  $\text{MCP}_{42}$ , although the protein and mineral composition may have changed. This could be related to the proposed structure of MCP and how it interacts with the phosphoserine residues of the individual caseins.

#### 4.3. Micellar Calcium Phosphate Adjustment: Insights from NMR Analysis

As established by  $^{31}\text{P}$  NMR, milk contains about 23 mM of inorganic phosphate ( $\text{P}_i$ ) and approximately 10 mM-phosphate esters, mainly as SerP residues of the caseins [42]. These phosphate assignments are clearly depicted as  $\delta \sim +1.9$  originating from  $\text{P}_i$  with, in general, a broad peak at approximately  $\delta = +3.2$  arising from SerP of the casein (Figure 5) [42]. Depending on the type of  $^{31}\text{P}$  NMR analysis, four types of phosphorus have been identified in literature including organic phosphorus from phosphoserine residues, organic phosphorus from serine to the MCP, inorganic phosphorus in the MCP and free inorganic phosphorus in the serum [43]. The MCP adjustment in our study appears to initially affect the width of the  $\text{P}_i$  peak (Figure 5) as it was wider at a higher MCP concentrations and then became narrower as the concentration of the MCP declined. This could be related to the types of  $\text{P}_i$  present in the MCP. Van Dijk [44] suggested that the MCP consisted of two parts—the stable arm, which crosslinks with SerP, and the unstable arm, which is in equilibrium with soluble salts in milk serum. Kolar et al. [45] extended on this suggestion and proposed that  $\text{P}_i$  appeared as three types including free inorganic phosphate in the serum, inorganic phosphate belonging to the unstable arm of the MCP and in the equilibrium with the serum  $\text{P}_i$ , and inorganic phosphate as a part of the stable arm of the MCP. Such a model has been termed  $\text{C}_2\text{-SerP}_3$  ion cluster and depicts 2 ‘free’ unstable and 2 stable arms firmly connecting 2 peptide chains [45]. It is likely that partial dissolution of the MCP would lead to solubilisation of the unstable MCP arms, which would not affect the integrity of the micelle greatly. However, once the stable arm is dissolved and SerP is exposed the micellar integrity appears to be compromised, which likely started to occur at MCP<sub>42</sub> (Figure 5D). At this point,  $\text{P}_o$  started to appear, indicated a greater mobility of SerP (Figure 5D). The peak at +3.2 ppm became the most prominent at the lowest MCP content. This is also confirmed by  $^1\text{H}$ -NMR (Figure 6) as the peaks in 2 identified regions (0.5–3.5 ppm and 5.5–9.0 ppm) started to change. The resonance around 1 ppm, which arises from the methyl protons of Ala, Leu, Ile and Thr residues, appeared to increase concomitant with the MCP decrease. At the same time, the peaks in the 5.5–9.0 ppm region, derived from amide main and side chain and aromatic side chain protons from caseins, started to become more distinct at MCP<sub>42–58</sub> (Figure 6D,E). The spectrum in the 7.5 and 8.5 ppm region has been assigned to the casein micelle backbone previously [46] and the peaks in this region were very broad but started to appear at MCP below 67% (Figure 6F). All of this indicates that either parts of the casein micelle became more mobile (resonated more) or the micelle lost its integrity, which resulted in greater resonance.

Increasing the MCP content by 13 or 29% had a rather minimal impact on the observed physical properties. However, it appears that the individual caseins are drawn from the soluble phase into the micellar structure. This resulted in the further immobilisation of organic phosphorus and widening of the  $\text{P}_i$  peak (Figure 5H,I), decline in the resonance associated with free amino acids depicted by  $^1\text{H}$ -NMR (Figure 6H,I) and decline in the concentration of non-sedimentable caseins (Figure 3). While it may be plausible that additional  $\text{P}_i$  could be incorporated into the unstable arm of the MCP, it is not clear how the individual caseins would be further incorporated into the casein micelle. This is especially in reference that the particle size did not change significantly thus one of the assumptions could be that they would be positioned somewhere in the interior. It is however evident that even increasing the MCP content above its native level would cause structural changes in the casein micelle including rise in side chains and aggregated  $\beta$ -sheets and decline in the  $\alpha$ -helical and  $\beta$ -turn structures (Table 3). How these structural changes may impact the properties and behaviour of the casein micelle under various processing conditions remains to be determined.

## 5. Conclusions

Several important physicochemical changes in milk proteins take place when the content of MCP in the casein micelle is altered. The casein micelle integrity did not appear substantially affected by the decline in MCP concentration following its adjustment down

to 42% of its original level, although the level of individual caseins increased in the serum phase of milk. The MCP content of 42% of the initial appears to be a minimum level to maintain the integrity of the casein micelle. While physical changes were not considerably noticeable above this level, the conformational changes in the casein micelle were substantially impacted by the adjustment. The MCP levels were also increased by adjustment at elevated pH although there appeared to be a limit to which additional Ca can be incorporated into the nanoclusters. This study provided some insights into the conformational and physicochemical changes in pasteurised milk with adjusted MCP.

**Supplementary Materials:** The following supporting information can be downloaded at: <https://www.mdpi.com/article/10.3390/foods13020322/s1>, Table S1: Changes in structural features of proteins in the Amide I region in MCP-adjusted skim milk samples as determined by Fourier transform Infrared Spectroscopy. MCP-adjusted skim milk samples containing from 7% (MCP<sub>7</sub>) to 129% (MCP<sub>129</sub>) of MCP relative to that of the control were obtained by either acidification or alkalisation followed by exhaustive dialysis against bulk milk. The spectra were obtained after the background adjustment. Figure S1. The original FTIR spectra (4000–650 cm<sup>-1</sup>) of MCP adjusted skim milk varied containing from 7% (MCP<sub>7</sub>) to 129% (MCP<sub>129</sub>) of MCP relative to that of the control achieved by either acidification or alkalisation followed by exhaustive dialysis against bulk milk.

**Author Contributions:** E.A. prepared this study, the research questions and the methodology and performed the experiments and formal analysis, visualisation, writing original draft. T.M. assisted with data analysis, review and editing, T.V. and T.H. supervised this study and provided critical feedback, analysis, review and editing and funding acquisition and resources. All authors have read and agreed to the published version of the manuscript.

**Funding:** This research was funded by both VU International Post-graduate Research Scholarship and FrieslandCampina.

**Institutional Review Board Statement:** Not applicable.

**Informed Consent Statement:** Not applicable.

**Data Availability Statement:** Data are contained within this article.

**Conflicts of Interest:** Thom Huppertz is employed by FrieslandCampina. The research was conducted without any relationships with the company that could be construed as potential conflicts of interest. The other authors declare that they have no conflict of interest or personal relationships that could have appeared to influence the work reported in this paper.

## References

1. Dalgleish, D.G.; Corredig, M. The structure of the casein micelle of milk and its changes during processing. *Annu. Rev. Food Sci. Technol.* **2012**, *3*, 449–467. [[CrossRef](#)] [[PubMed](#)]
2. Holt, C. Structure and stability of bovine casein micelles. *Adv. Protein Chem.* **1992**, *43*, 63–151. [[CrossRef](#)] [[PubMed](#)]
3. Gaucheron, F. The minerals of milk. *Reprod. Nutr. Dev.* **2005**, *45*, 473–483. [[CrossRef](#)]
4. Schäfer, J.; Mesch, I.; Atamer, Z.; Nöbel, S.; Kohlus, R.; Hinrichs, J. Calcium reduced skim milk retentates obtained by means of microfiltration. *J. Food Eng.* **2019**, *247*, 168–177. [[CrossRef](#)]
5. Pyne, G.T.; McGann, T.C.A. The colloidal phosphate of milk: II. Influence of citrate. *J. Dairy Res.* **1960**, *27*, 9–17. [[CrossRef](#)]
6. Shalabi, S.I.; Fox, P.F. Influence of pH on the rennet coagulation of milk. *J. Dairy Res.* **1982**, *49*, 153–157. [[CrossRef](#)]
7. Anema, S.G. Role of colloidal calcium phosphate in the acid gelation properties of heated skim milk. *Food Chem.* **2009**, *114*, 161–167. [[CrossRef](#)]
8. Silva, N.N.; Piot, M.; de Carvalho, A.F.; Violleau, F.; Fameau, A.L.; Gaucheron, F. pH-induced demineralization of casein micelles modifies their physico-chemical and foaming properties. *Food Hydrocoll.* **2013**, *32*, 322–330. [[CrossRef](#)]
9. Zhao, Z.; Corredig, M. Serum composition of milk subjected to re-equilibration by dialysis at different temperatures, after pH adjustments. *J. Dairy Sci.* **2016**, *99*, 2588–2593. [[CrossRef](#)]
10. Huppertz, T.; Lambers, T.T. Influence of micellar calcium phosphate on in vitro gastric coagulation and digestion of milk proteins in infant formula model systems. *Int. Dairy J.* **2020**, *107*, 104717. [[CrossRef](#)]
11. Kommineni, A.; Sunkesula, V.; Marella, C.; Metzger, L.E. Calcium-reduced micellar casein concentrate-physicochemical properties of powders and functional properties of the dispersions. *Foods* **2022**, *11*, 1377. [[CrossRef](#)] [[PubMed](#)]
12. Fox, P.F.; Hoynes, M.C.T. Heat stability of milk: Influence of colloidal calcium phosphate and  $\beta$ -lactoglobulin. *J. Dairy Res.* **1975**, *42*, 427–435. [[CrossRef](#)]

13. Singh, H.; Fox, P.F. Heat stability of milk: Influence of colloidal and soluble salts and protein modification on the pH-dependent dissociation of micellar  $\kappa$ -casein. *J. Dairy Res.* **1987**, *54*, 523–534. [[CrossRef](#)]
14. Anema, S.G.; Li, Y. Further studies on the heat-induced, pH-dependent dissociation of casein from the micelles in reconstituted skim milk. *LWT-Food Sci. Technol.* **2000**, *33*, 335–343. [[CrossRef](#)]
15. Ahmadi, E.; Vasiljevic, T.; Huppertz, T. Influence of pH on heat-induced changes in skim milk containing various levels of micellar calcium phosphate. *Molecules* **2023**, *28*, 6847. [[CrossRef](#)] [[PubMed](#)]
16. Jenness, R.; Koops, J. Preparation and properties of a salt solution which simulates milk ultrafiltrate. *Neth. Milk Dairy J.* **1962**, *16*, 153–164.
17. Griffin, M.C.A.; Griffin, W.G. A simple turbidimetric method for the determination of the refractive index of large colloidal particles applied to casein micelles. *J. Colloid. Interface Sci.* **1985**, *104*, 409–415. [[CrossRef](#)]
18. Grewal, M.K.; Chandrapala, J.; Donkor, O.; Apostolopoulos, V.; Stojanovska, L.; Vasiljevic, T. Fourier transform infrared spectroscopy analysis of physicochemical changes in UHT milk during accelerated storage. *Int. Dairy J.* **2017**, *66*, 99–107. [[CrossRef](#)]
19. Markoska, T.; Daniloski, D.; Vasiljevic, T.; Huppertz, T. Structural changes of  $\beta$ -casein induced by temperature and pH analysed by nuclear magnetic resonance, Fourier-transform infrared spectroscopy, and chemometrics. *Molecules* **2021**, *26*, 7650. [[CrossRef](#)]
20. Bijl, E.; Huppertz, T.; Valenberg, H.V.; Holt, C. A quantitative model of the bovine casein micelle: Ion equilibria and calcium phosphate sequestration by individual caseins in bovine milk. *Eur. Biophys. J.* **2019**, *48*, 45–59. [[CrossRef](#)]
21. Holt, C.; Davies, D.T.; Law, A.J. Effects of colloidal calcium phosphate content and free calcium ion concentration in the milk serum on the dissociation of bovine casein micelles. *J. Dairy Res.* **1986**, *53*, 557–572. [[CrossRef](#)]
22. Ono, T.; Ohotawa, T.; Takagi, Y. Complexes of casein phosphopeptide and calcium phosphate prepared from casein micelles by tryptic digestion. *Biosci. Biotechnol. Biochem.* **1994**, *58*, 1376–1380. [[CrossRef](#)]
23. Lyu, P.C.; Sherman, J.C.; Chen, A.; Kallenbach, N.R. Alpha-helix stabilization by natural and unnatural amino acids with alkyl side chains. *Proc. Natl. Acad. Sci. USA* **1991**, *88*, 5317–5320. [[CrossRef](#)]
24. Gonzalez-Jordan, A.; Thomar, P.; Nicolai, T.; Dittmer, J. The effect of pH on the structure and phosphate mobility of casein micelles in aqueous solution. *Food Hydrocoll.* **2015**, *51*, 88–94. [[CrossRef](#)]
25. Sørensen, H.; Mortensen, K.; Sørland, G.H.; Larsen, F.H.; Paulsson, M.; Ipsen, R. Dynamic ultra-high pressure homogenisation of milk casein concentrates: Influence of casein content. *IFSET* **2014**, *26*, 143–152. [[CrossRef](#)]
26. Du, Z.; Xu, N.; Yang, Y.; Li, G.; Tai, Z.; Li, N.; Sun, Y. Study on internal structure of casein micelles in reconstituted skim milk powder. *Int. J. Biol. Macromol.* **2023**, *224*, 437–452. [[CrossRef](#)] [[PubMed](#)]
27. Rollema, H.S.; Brinkhuis, J.A. A  $^1\text{H}$ -NMR study of bovine casein micelles; influence of pH, temperature and calcium ions on micellar structure. *J. Dairy Res.* **1989**, *56*, 417–425. [[CrossRef](#)] [[PubMed](#)]
28. Lemos, A.T.; Goodfellow, B.J.; Delgadillo, I.; Saraiva, J.A. NMR metabolic composition profiling of high pressure pasteurized milk preserved by hyperbaric storage at room temperature. *Food Control.* **2022**, *134*, 108660. [[CrossRef](#)]
29. Horne, D.S. Milk Proteins: Casein, Micellar Structure. In *Encyclopedia of Dairy Sciences*, 2nd ed.; Fuquay, J.W., Ed.; Academic Press: Cambridge, MA, USA; Elsevier: Amsterdam, The Netherlands, 2011; pp. 772–779.
30. de Kruijff, C.G.; Huppertz, T.; Urban, V.S.; Petukhov, A.V. Casein micelles and their internal structure. *Adv. Colloid Interface Sci.* **2012**, *171*, 36–52. [[CrossRef](#)]
31. Holt, C. An equilibrium thermodynamic model of the sequestration of calcium phosphate by casein micelles and its application to the calculation of the partition of salts in milk. *Eur. Biophys. J.* **2004**, *33*, 421–434. [[CrossRef](#)]
32. Holt, C.; van Kemenade, M.J.; Nelson, L.S.; Sawyer, L.; Harries, J.E.; Bailey, R.T.; Hukins, D.W. Composition and structure of micellar calcium phosphate. *J. Dairy Res.* **1989**, *56*, 411–416. [[CrossRef](#)]
33. Thomsen, J.K.; Jakobsen, H.J.; Nielsen, N.C.; Petersen, T.E.; Rasmussen, L.K. Solid-state magic-angle spinning  $^{31}\text{P}$ -NMR studies of native casein micelles. *Eur. J. Biochem.* **1995**, *230*, 454–459. [[CrossRef](#)] [[PubMed](#)]
34. Bak, M.; Rasmussen, L.K.; Petersen, T.E.; Nielsen, N.C. Colloidal calcium phosphates in casein micelles studied by slow-speed-spinning  $^{31}\text{P}$  magic angle spinning solid-state nuclear magnetic resonance. *J. Dairy Sci.* **2001**, *84*, 1310–1319. [[CrossRef](#)] [[PubMed](#)]
35. Hindmarsh, J.P.; Watkinson, P. Experimental evidence for previously unclassified calcium phosphate structures in the casein micelle. *J. Dairy Sci.* **2017**, *100*, 6938–6948. [[CrossRef](#)] [[PubMed](#)]
36. Munyua, J.K.; Larsson-Raznikiewicz, M. The influence of  $\text{Ca}^{2+}$  on the size and light scattering properties of casein micelles 1.  $\text{Ca}^{2+}$  removal. *Milchwissenschaft* **1980**, *35*, 604–606.
37. Dalgleish, D.G. Casein micelles as colloids: Surface structures and stabilities. *J. Dairy Sci.* **1998**, *81*, 3013–3018. [[CrossRef](#)]
38. Srinivasan, M.; Lucey, J.A. Effects of added plasmin on the formation and rheological properties of rennet-induced skim milk gels. *J. Dairy Sci.* **2002**, *85*, 1070–1078. [[CrossRef](#)]
39. Horne, D.S.; Lucey, J.A. Revisiting the temperature dependence of the coagulation of renneted bovine casein micelles. *Food Hydrocoll.* **2014**, *42*, 75–80. [[CrossRef](#)]
40. Byler, D.M.; Farrell, J.H.M.; Susi, H. Raman spectroscopic study of casein structure. *J. Dairy Sci.* **1988**, *71*, 2622–2629. [[CrossRef](#)]
41. Grewal, M.K.; Vasiljevic, T.; Huppertz, T. Influence of calcium and magnesium on the secondary structure in solutions of individual caseins and binary casein mixtures. *Int. Dairy J.* **2021**, *112*, 104879. [[CrossRef](#)]

42. Belton, P.S.; Lyster, R.L.; Richards, C.P. The  $^{31}\text{P}$  nuclear magnetic resonance spectrum of cows' milk. *J. Dairy Res.* **1985**, *52*, 47–54. [[CrossRef](#)]
43. Nogueira, M.H.; Ben-Harb, S.; Schmutz, M.; Doumert, B.; Nasser, S.; Derensy, A.; Karoui, R.; Delaplace, G.; Peixoto, P.P.S. Multiscale quantitative characterization of demineralized casein micelles: How the partial excision of nan-clusters leads to the aggregation during rehydration. *Food Hydrocoll.* **2020**, *105*, 105778. [[CrossRef](#)]
44. van Dijk, H.J.M. The properties of casein micelle. 1. The nature of the micellar calcium phosphate. *Neth. Milk Dairy J.* **1990**, *44*, 65–81.
45. Kolar, Z.I.; Verburg, T.G.; van Dijk, H.J. Three kinetically different inorganic phosphate entities in bovine casein micelles revealed by isotopic exchange method and compartmental analysis. *J. Inorg. Biochem.* **2002**, *90*, 61–66. [[CrossRef](#)]
46. Lamanna, R.; Braca, A.; Di Paolo, E.; Imparato, G. Identification of milk mixtures by  $^1\text{H}$  NMR profiling. *Magn. Reson. Chem.* **2011**, *49*, S22–S26. [[CrossRef](#)] [[PubMed](#)]

**Disclaimer/Publisher's Note:** The statements, opinions and data contained in all publications are solely those of the individual author(s) and contributor(s) and not of MDPI and/or the editor(s). MDPI and/or the editor(s) disclaim responsibility for any injury to people or property resulting from any ideas, methods, instructions or products referred to in the content.